

# Advancing Solar Power Predictions: Exploring Neural Network Architecture through Transfer Function and Hidden Layer Analysis

Siti Nur Afifah Mohd Suhaimi<sup>1</sup>, Nor Aira Zambri<sup>1,\*</sup>, Norhafiz Salim<sup>2</sup>, Farahiyah Mustafa<sup>1</sup>, Mohd Nasri Jasmie<sup>3</sup>

<sup>1</sup> Department of Electrical Engineering Technology, Fakulti Teknologi Kejuruteraan Elektrikal, Universiti Tun Hussien Onn Malaysia, UTHM Kampus Pagoh, Hab Pendidikan Tinggi Pagoh, KM 1, Jalan Panchor, 84600 Panchor, Johor, Malaysia

<sup>2</sup> Faculty of Electrical Engineering, Universiti Teknikal Malaysia Melaka, Jalan Hang Tuah Jaya, Durian Tunggal, Melaka, 76100, Malaysia

<sup>3</sup> Eramaz (M) Sdn. Bhd. Unit 5-1, Pintas Square, Jalan Penampang Bypass, 88200 Kota Kinabalu, Sabah, Malaysia

## ARTICLE INFO

### Article history:

Received 8 April 2025

Received in revised form 21 July 2025

Accepted 23 September 2025

Available online 7 October 2025

## ABSTRACT

Artificial Neural Network (ANN) models have demonstrated robustness in capturing variations in the input-output relationship between weather parameters and photovoltaic (PV) output power. However, despite their success in solar power forecasting, the challenge of determining the optimal architecture. This study aims to enhance the precision of photovoltaic (PV) output prediction by focusing on four inputs where irradiance, ambient temperature, PV module temperature, and humidity. The primary objective is to discern the most effective neural network architecture, specifically identifying the optimal number of neurons and hidden layers. The study employs the Multilayer Perceptron (MLP) technique, a type of ANN, to develop the model. Training shows that varying the number of neurons in the hidden layer, explicitly using 18 neurons, leads to optimal performance. Furthermore, it compares the best activation function between different activation functions, including linear, Hyperbolic Tangent Sigmoid (tan-sig), and Logistic Sigmoid (log-sig). The analysis concludes that the best activation function is achieved when the MLP model is designed using log-sig- linear- log-sig in the hidden layer with a structure of (4-18-18-18-4) for 560 data entries, using the MATLAB Deep Learning Toolbox. The results obtained from the neural network are thoroughly analyzed, indicating that using 18 neurons across the 3 hidden layers proves to be the most effective configuration for training, testing, and validation. This configuration yields minimal Root Mean Square Error (RMSE), emphasizing its strong performance in this study. The obtained result from this study, highlights the significance of fine-tuning neural network architecture for accurate and reliable solar power forecasting, contributing to advancements in renewable energy applications.

### Keywords:

ANN; MLP; prediction; MATLAB; PV power output; transfer function; RMSE

## 1. Introduction

The demand for renewable energy is increasing daily, indicating a positive shift towards a sustainable future and a reduced reliance on non-renewable energy sources globally. Solar energy is an extensive, abundant, cost-free, and environmentally friendly renewable source. Because of these inherent qualities, the world is currently engaged in research and exploration to identify the most optimized methods for harnessing this abundant energy resource [1]. The

\* Corresponding author.

E-mail address: [aira@uthm.edu.my](mailto:aira@uthm.edu.my)

International Energy Agency (IEA) has announced that the worldwide production of solar photovoltaic (PV) is poised for substantial expansion in 2022, anticipating a growth of over 70% in manufacturing capacity [2]. According to the Malaysia Energy Statistics Handbook 2020, the total installed solar capacity by the end of 2019 was 1056.3 MW, with 948.6 MW in Peninsular Malaysia, 107.6 MW in Sabah, and 0.1 MW in Sarawak [3]. This data reflects a notable increase in installations compared to the figures from five years prior in Malaysia.

The efficiency and performance of a solar photovoltaic (PV) system are contingent upon a range of environmental factors [4]. These elements significantly influence the output of the PV panels, determining how effectively the system converts sunlight into electricity. To improve the planning and operation of PV power generation plants, forecasting methods are used to mitigate the imbalance of PV power [5]. Accurate PV power forecasting employs various time-series methods, including deep-learning and machine-learning algorithms, to rapidly forecast PV power generation output, facilitating prompt responses to equipment and panel defects, making it particularly effective for swift PV power generation forecasting [6]. In addition, forecasting prediction is essential for the efficient and effective integration of solar energy into the power grid, promoting sustainability, reducing costs, and ensuring the reliability of energy systems.

### *1.1 Type of forecasting*

In recent forecasting methods, the two primary approaches are direct and indirect methods [7]. Direct forecasting entails predicting target variables without considering the underlying relationships between input and output variables. This paper directly emphasizes the off-grid solar system as an example of direct solar power output prediction. The approach involves using weather parameters as inputs and employing a Feed-Forward Multi-Layer Perceptron (MLP) Artificial Neural Network (ANN) model for PV power forecasting, facilitated by MATLAB's Deep Learning Toolbox [5]. In the context of direct prediction, a day-ahead solar power forecasting method adopts an innovative hybrid classification-regression forecasting engine to enhance solar power forecast accuracy [8].

Conversely, indirect forecasting involves creating a model that captures the relationships between input and target variables [9], [10]. This study develops a model using ten years of solar data and other meteorological parameters recorded at 1-hour intervals to enhance the efficiency of predicting solar irradiance and PV power output [11]. Another indirect approach involves using a sole input solar irradiance map integrated with a Generative Adversarial Network (GAN) to accurately predict solar irradiance, subsequently indirectly forecasting PV power output through an irradiance-to-power model [12].

The idea of this study where the irradiance (IR), ambient temperature ( $A_{Temp}$ ), PV module temperature ( $PV_{Temp}$ ), and humidity as inputs for predicting various output parameters, including maximum power output ( $P_{max}$ ), voltage at maximum power ( $V_{mp}$ ), current at maximum power ( $I_{mp}$ ), and open-circuit voltage ( $V_{oc}$ ) is typically associated with a type of forecasting known as indirect or model-based forecasting

### *1.2 Previous studies*

An artificial neural network (ANN) is a computational model inspired by the structure and functioning of biological neural networks, such as the human brain [13],[14]. It is a mathematical framework composed of interconnected nodes, called artificial neurons or "nodes," organized in layers. The basic building block of an artificial neuron is a mathematical function that takes input signals, applies weights to them, performs a calculation, and produces an output signal [14]. These

artificial neurons are typically organized into layers with an input layer, one or more hidden layers, and an output layer [15].

During the training phase, the weights are adjusted repetitively through a process known as backpropagation, where the network learns from labeled training data to minimize the difference between its predicted outputs and the desired outputs [13], [16]. ANN excels at pattern recognition, classification, regression, and other tasks that involve learning from examples or data. They can approximate complex, non-linear relationships and generalize from the training data to make predictions or decisions on new, unseen data. They are fundamental to machine learning and are often used as the core component in deep learning models.

ANN has been effectively used in various fields, including forecasting, short-term load prediction, etc. The ideal time horizon for utilizing the ANN model for prediction is between 1 and 24 hours into the future [17]. ANN can deliver superior results even during overcast conditions, a performance that linear statistical models cannot achieve [18].

There are various types of ANN architectures, including Multi-Layer Perceptron (MLP), the most widely used and essential form of ANN [19]. In an MLP, neurons are organized feedforward, meaning the information flows from the input layer through the hidden layers to the output layer [20],[21]. The "input" parameter represents the input data used for training, while the "output" parameter corresponds to the corresponding outputs associated with the provided inputs. MLPs are known for their ability to learn complex patterns and are often used for tasks such as classification and regression. Table 1 summarizes the ANN models used in different studies and their respective tests and parameters.

**Table 1**  
Summary of studies employing ANN

Author	Input variables	Neural Network	Observation
Mahmoud Jaber et.al., (2022) [4]	Cell temperature, irradiance, fill factor, short circuit current, open-circuit voltage, maximum power, and the product of Voc and Isc	ANN- GRNN	This author presents the comparison prediction performance for efficiency, IV curve, and fill factor for 6 different types of PV modules by using ANN combined with generalized regression neural network (GRNN) and MATLAB to train and test the data. The results show the most efficient is mono and the least in thin film modules.
Aminu Bugaje et.al., (2021) [5]	Temperature, diffuse irradiation, direct irradiation, humidity, the azimuth angle of the sun and zenith angle of the sun	ANN-MLP	The ANN model was employed for predicting the power output of an off-grid solar system. Various ANN model scenarios were created by altering the number of input features. The findings indicate that the ANN model with six input features (6-30-1) demonstrated superior accuracy. Nevertheless, the ANN model with three input features (3-30-1) still yielded a noteworthy level of accuracy, though slightly less than its counterpart with six input features.
Pedro Lara-Benítez et. al., (2023) [10]	Solar irradiance, cloud coverage	MLP, LSTM, CNN, and Transformer network	The findings indicate that MLP and CNN exhibit the highest accuracy and a notable capacity to adapt to training data. Through an exhaustive grid search parametrization involving 90 models for each dataset, MLP emerged as the top-performing model, particularly excelling in scenarios with lower irradiance variability. The simplicity of the MLP architecture facilitates swift convergence and

			efficient adaptation to concept drifts, especially in situations where the overly complex problem.
Fatih et. al., (2021) [22]	indigenous models: longitude, sunshine durations, precipitation, and wind speed widespread models: latitude, sunshine durations, and mean daily maximum air temperature.	ANN	The hybrid model integrates feature selection and ANN properties to enhance accuracy. The proposed generic ANN model is trained using world weather data. The optimization parameters are customized to improve prediction accuracy.
Anass Zaaoumi et. al., (2020) [23]	Direct normal irradiation, hour of the year, hour of the day, ambient temperature, relative humidity, wind speed, ambient pressure, previous hourly energy production	ANN-MLP	The study's results reveal that the three-layer MLP model best estimates hourly electric energy generation, particularly with 22 hidden neurons. The developed ANN model is well-suited for estimating the energy production of a solar power plant equipped with parabolic trough collectors.
Ines Tavares et. al., (2022) [24]	Output PV data system installed on the 15 roofs of residential buildings.	MLP- ANN & DNN-CNN-RNN	The comparison and discussion of forecasting results between the MLP with ANN and Deep Neural Networks (DNN) combined with a Convolution Neural Network (CNN) and a Recurrent Neural Network (RNN). ANN is more capable of predicting PV generation with a lower forecasting error. This implies that, in the context of the study or application, ANN outperforms the alternative neural network technique with a parameter of 3 layers, 10 hidden neurons of 1 hidden layer, providing more accurate and reliable predictions for PV generation.

According to Table 1, various findings on neural network output have been documented in previous research. In alignment with the suggestion in reference [10], [24] this study will utilize MLP-ANN, which exhibits the highest accuracy. The research focuses on adjusting the number of neurons and layers in the hidden layer, specifically exploring configurations with 2 and 3 layers. This study focuses on how the factor significantly impacts network learning and prediction abilities.

To optimize neural network performance, the study includes diverse transfer functions in the hidden layer, such as Hyperbolic Tangent Sigmoid, Logistic Sigmoid, and Linear. The significance of various activation functions is emphasized, and a detailed analysis of their impact, individually and in combinations across two and three hidden layers, is conducted. The objective is to identify the most effective setup during training, testing, and validation to minimize errors and improve accuracy in predicting PV power output.

In summary, the study aims to refine neural network predictions by strategically considering activation functions, neuron layer configurations, and transfer functions, providing valuable insights for advancing solar energy forecasting.

## 2. Methodology

### 2.1 Overview of the experimental setup and data collection

This section provides a detailed explanation of the implemented methodology, starting with the data collection for both input and output of solar data on the rooftop of the building. The subsequent step involves defining the number of neurons, hidden layers, and transfer functions in both the hidden and output layers. Various activation functions are tested during this phase. If the system

proves unstable or exhibits errors, it undergoes re-testing until the predetermined objectives are satisfactorily met.

In this study, data collection involves utilizing four inputs and four outputs of the PV module. The inputs include solar irradiance (IR) data, humidity, ambient temperature ( $A_{Temp}$ ), and PV module temperature ( $PV_{Temp}$ ). At the same time, the outputs consist of the voltage at the maximum point ( $V_{mp}$ ), current at the maximum point ( $I_{mp}$ ), power at the maximum point ( $P_{max}$ ), and open-circuit voltage ( $V_{oc}$ ) of the PV module. Raw data was gathered over six days, generating a dataset of 580 entries, employing an irradiance data logger, solar power meter, and humidity meter.

Subsequently, all collected data undergoes a normalization process, scaling values from 0 to 1. This normalization step is crucial before initiating the training, testing, and validation phases of an ANN, as it enhances stability, convergence, and optimal model performance. The graphical structure of the proposed model development is illustrated in Figure 1.

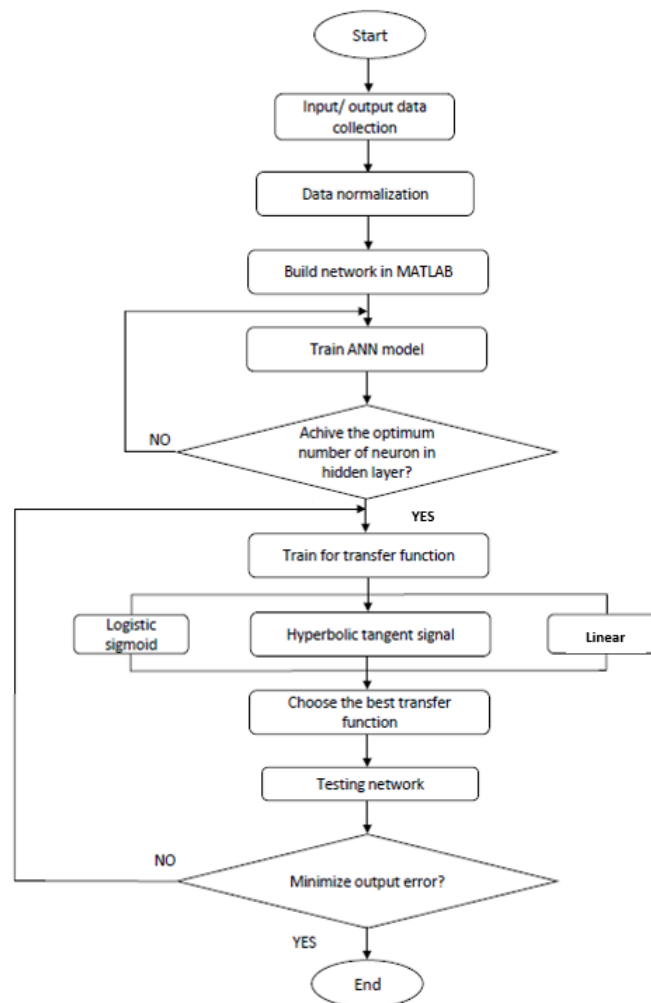


**Fig. 1.** Flowchart of the system.

## 2.2 Designing the ANN model

The forecasting model capitalizes on the benefits of using an MLP known for its relative simplicity. MLP employs the error Back Propagation training algorithm to minimize the mean squared error, reducing the disparity between the desired and actual model output with each presentation of input data [5], [20]. The choice of MLP is driven by its ability to handle data inconsistencies, a feature

particularly crucial when confronted with the non-linearities introduced by fluctuating weather conditions. This is achieved by incorporating at least one hidden layer with a non-linear activation function, effectively addressing the challenges posed by the non-linear nature of the data [5], [10].

For the training of the ANN model, the normalized data, comprising the generated PV output, serves as the target data. Simultaneously, weather data acts as input training features. The MLP-ANN model is developed and trained until an optimal model accuracy is attained, as indicated by sufficiently low Root Mean Squared Error (RMSE) values. The formula of RMSE at Eq. (1).

$$RMSE = \sqrt{\frac{1}{n} \sum_{i=1}^n (t_i - \hat{t}_i)^2} \quad (1)$$

To simplify the training of the ANN model, data pre-processing is necessary. Given the dependence of PV output on seasonal boundary conditions, it becomes essential to eliminate seasonal variation from the input data. This pre-processing is achieved using the MATLAB built-in function '*dividerand*', which randomizes the training dataset into three sets with corresponding random indices [5]. The matrices used for grouping the 580 data entries in MATLAB during the training stage are as follows:

- The training set 70% ratio, which comprises 406 data entries.
- The testing set 15% ratio consists of 87 data entries.
- The remaining 15% of the validation set includes 87 data entries.

To attain the optimal fit, the ANN models underwent training using the Levenberg-Marquardt Back Propagation algorithm which the network underwent training for 1000 epochs. This involved continuously adjusting the weights of the hidden and output nodes until the predicted model output was closely aligned with the target outputs during the training stage. MATLAB's built-in transfer functions, specifically linear, Hyperbolic Tangent Sigmoid (logsig), and Logistic Sigmoid (tansig) were employed in this study, shown in Figure 2. The ANN-developed performance and accuracy were evaluated through the RMSE analysis.

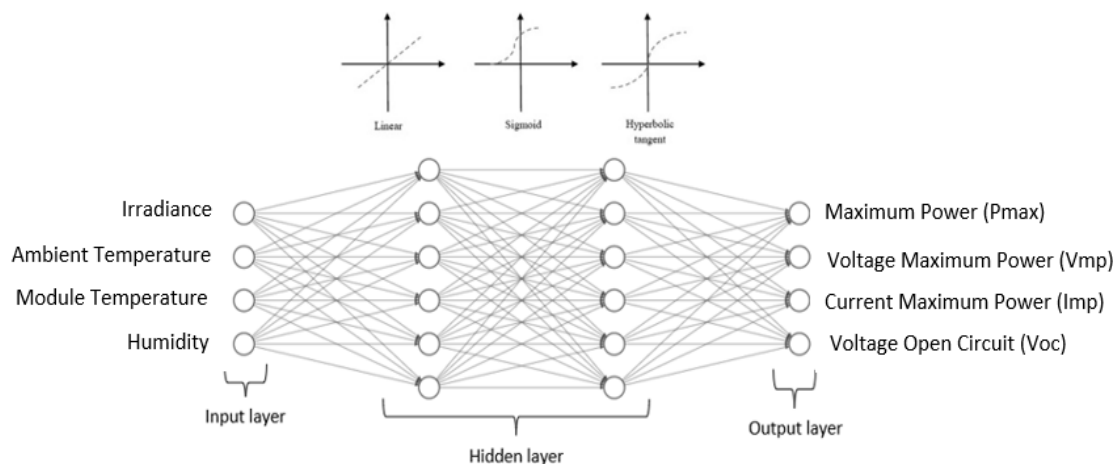


**Fig. 2.** The four-layer architecture of MLP with different activation functions.

**Table 2**

Data for input and output in 2 hours

11:00 AM	34.76	15.87	2.19	21.70	618	50	61.0	32.5
11:05 AM	36.13	16.13	2.24	21.74	642	52	60.8	32.9
11:10 AM	36.02	15.87	2.27	21.74	647	52	58.5	34.2
11:15 AM	36.06	15.28	2.36	21.74	649	50	66.7	31.8
11:20 AM	35.76	15.28	2.34	21.67	656	52	65.8	32.1
11:25 AM	38.01	15.39	2.47	21.70	649	52	61.5	32.1
11:30 AM	37.68	15.83	2.38	21.70	668	51	61.3	32.6
11:35 AM	39.20	15.87	2.47	22.01	664	50	58.5	33.8
11:40 AM	38.80	15.46	2.51	21.01	611	50	57.5	33.9
11:45 AM	28.48	16.09	1.77	21.15	671	49	44.4	39.7
11:50 AM	27.95	15.79	1.77	21.15	683	50	45.2	39.7
11:55 AM	39.05	15.02	2.60	21.97	666	50	45.8	39.7
12:00 PM	39.48	15.79	2.50	22.01	669	51	45.2	39.7
12:05 PM	42.56	15.31	2.78	21.97	742	53	45.1	39.5
12:10 PM	42.61	15.90	2.68	21.97	774	55	44.8	39.1
12:15 PM	42.01	15.39	2.73	21.70	451	53	46.9	39.7
12:20 PM	42.71	15.31	2.79	21.74	443	49	47.0	39.7
12:25 PM	41.00	15.31	2.73	21.74	705	51	47.5	39.7
12:30 PM	41.84	15.90	2.65	21.74	751	54	46.3	30.5
12:35 PM	34.75	15.31	2.27	21.74	816	55	47.5	39.7
12:40 PM	45.16	15.31	2.84	21.74	572	57	48.4	39.7
12:45 PM	52.33	15.39	3.40	22.16	370	52	48.3	37.8
12:50 PM	51.76	15.09	3.43	22.16	877	48	47.1	37.9
12:55 PM	51.11	14.90	3.43	22.16	853	54	49.1	38.0
1:00 PM	50.97	14.86	3.43	22.08	321	53	48.9	38.2

The data of irradiance (IR), PV temperature ( $PV_{Temp}$ ), Humidity, Ambient Temperature ( $A_{Temp}$ ), maximum power output ( $P_{max}$ ), voltage at maximum power ( $V_{mp}$ ), current at maximum power ( $I_{mp}$ ), and open-circuit voltage ( $V_{oc}$ ). These values in Table 2 represent a sample of data collected over 2 hours, as indicated in the study.

In Figure 3, the trend illustrates the relationship between the input and output of the PV data. The data in this figure is obtained from the normalized values of the 2-hour sample from Table 2, showcasing the correlation between each input and output. The data indicates that irradiance plays a pivotal role in enhancing the performance of solar panels, as an increase in solar radiation from 11 am to 1 pm correlates with higher  $P_{max}$ ,  $V_{mp}$ ,  $I_{mp}$ , and  $V_{oc}$ . Conversely, elevated temperatures, indicated by both  $PV_{Temp}$  and  $A_{Temp}$ , have an adverse impact on these parameters, resulting in decreased efficiency. While the influence of humidity appears less prominent, there is a suggestion that higher humidity levels might contribute to a slight reduction in  $P_{max}$ ,  $V_{mp}$ ,  $I_{mp}$ , and  $V_{oc}$ . This observation aligns with findings in [25]. Recognizing these trends is crucial for optimizing the overall efficiency of solar power systems in various environmental conditions.

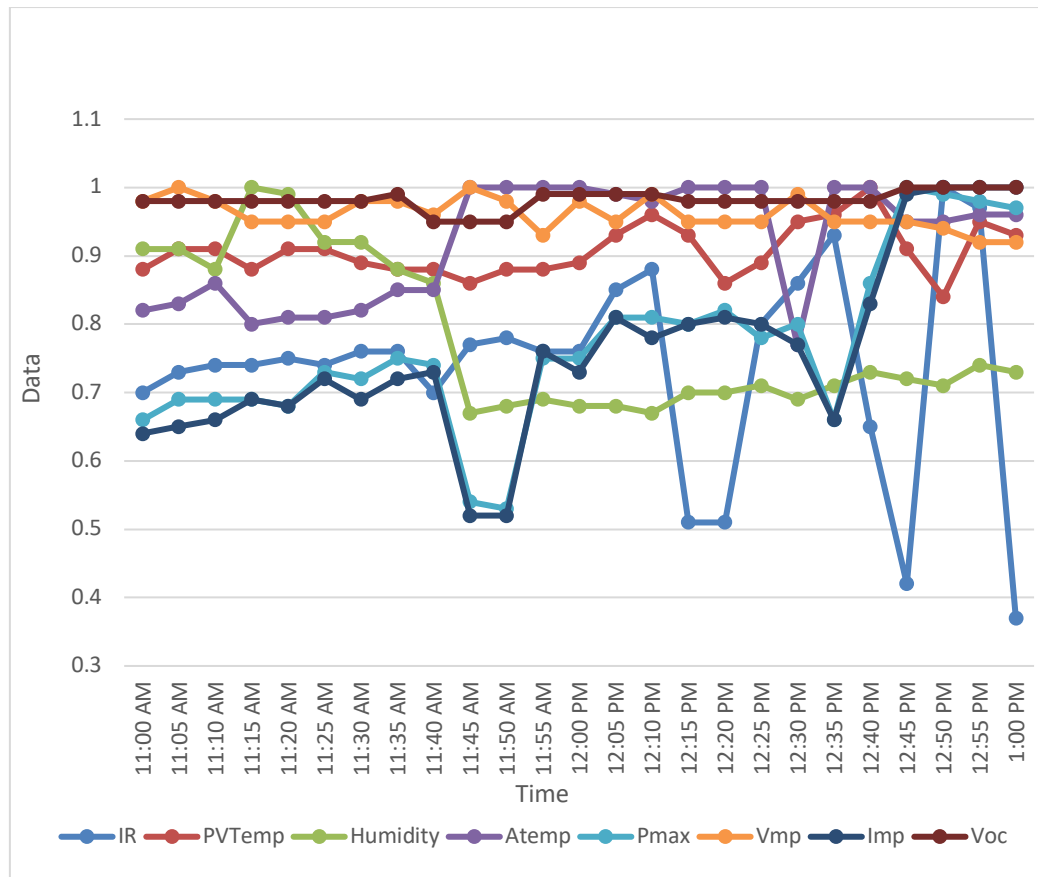


Fig. 3. Relationship of input and output of PV data with normalized data

### 3. Result and discussion

The results were obtained from the PV dataset, which consisted of 580 entries collected over six days. This dataset includes measurements for both input and output, ranging from morning to evening. Selecting the number of hidden neurons represents the initial step in developing the ANN model. Throughout this process, the overall performance of the hidden neurons was evaluated by incrementing one neuron at a time over 20 runs. The most effective architecture among all tested ANN models is the one that produces the best results for the training, test, and validation dataset.

Table 3

Average performance obtained from different numbers of neurons

Number Of Hidden Neurons	Epoch	Train	Test	Validation	Number Of Hidden Neurons	Epoch	Train	Test	Validation
8	24	0.9639	0.9617	0.9484	15	40	0.9910	0.9630	0.9735
9	37	0.9747	0.9426	0.9617	16	78	0.9949	0.9555	0.9723
10	31	0.9809	0.9384	0.9433	17	82	0.9939	0.7867	0.9736
11	28	0.9785	0.9360	0.965	18	33	<b>0.9998</b>	<b>0.9636</b>	<b>0.9764</b>
12	58	0.9855	0.9772	0.9742	19	25	0.9843	0.8697	0.9620
13	29	0.9851	0.9281	0.9843	20	24	0.9860	0.9423	0.9600
14	43	0.9898	0.9343	0.9663	21	21	0.9871	0.9715	0.9523



In this paper, a transfer function of log-sig-log-sig was employed with four hidden layers: the first layer for input, the second and third layers for the transfer function, and the last layer for output. Table 3 summarizes the peak performances achieved in the dataset over 20 runs. The table indicates that the optimal number of hidden neurons is 33, with training accuracy at 0.9998, testing accuracy at 0.9636, and validation accuracy at 0.9764. The objective is to identify the best architecture that accurately represents the relationship between transfer functions in 2 hidden layers and 3 hidden layers with different transfer functions.

**Table 4**

Different types of transfer functions with 2 and 3 hidden layers.

No	Type Of Transfer Function	Epoch	Train	Test	Validation
1	Log-sig – Log-sig	33	0.9918	0.9636	0.9764
2	Log-sig – Log-sig – Log-sig	42	0.9980	0.9335	0.9794
3	Log-sig – Linear	47	0.9697	0.9253	0.9253
4	<b>Log-sig – Linear – Log-sig</b>	<b>37</b>	<b>0.9907</b>	<b>0.9615</b>	<b>0.9781</b>
5	Linear– Log-sig	36	0.9750	0.9499	0.9596
6	Linear – Log-sig – Linear	21	0.9652	0.9400	0.9356
7	Linear – Linear	4	0.9151	0.8975	0.9480
8	Tan-sig – Linear	30	0.9655	0.9630	0.9589
9	Tansig – Linear – Tan-sig	23	0.9906	0.8835	0.9595
10	Tan-sig – Tan-sig	16	0.98328	0.9655	0.9437

Several tests have been performed in the current study to select the transfer function by varying the number of neurons using a constructive approach, using 18 layers of neurons in the hidden layer. Therefore, the 3 hidden layers of Log-sig with linear MLP activation give the best training, test, and validation results compared to other activation functions in this project. The comparison RMSE for each type of transfer function will be explained in detail. Therefore, the result in Table 4, combining 18 layers of neurons with a 3-hidden-layer Log-sig-Linear-Log-sig transfer function at epoch 37, can be considered a suitable architecture for accurately estimating PV power output on an hourly scale. The regression plots of Log-sig-Linear-Log-sig transfer function measured and predicted ANN model energy for PV power output for the training is 0.9907, test is 0.9615, and validation achieve 0.9781 are presented in Figure 4.

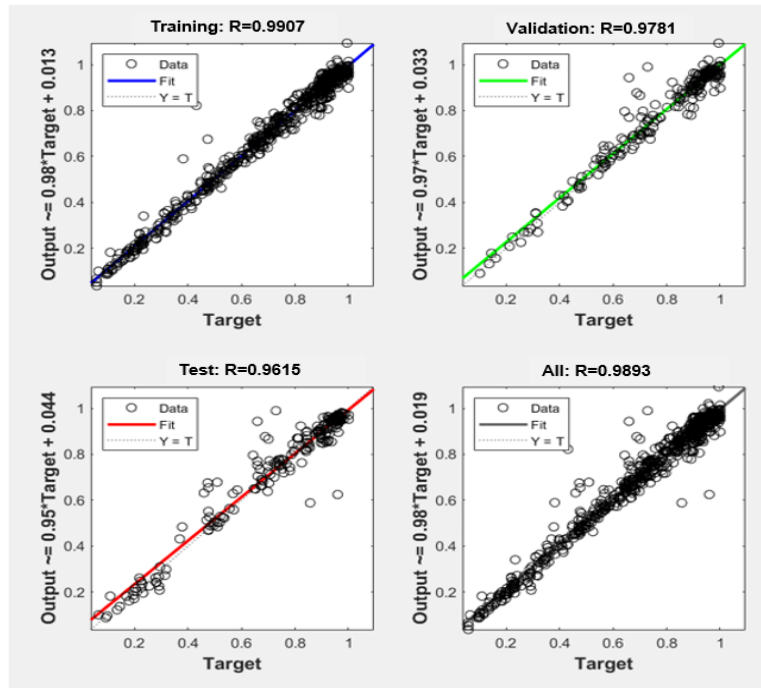


**Fig. 4.** ANN model energy for PV power output for the training, test, and validation dataset for Log-sig-Linear-Log-sig transfer function

### 3.1 Result in RMSE for all types of transfer functions

The actual data were normalized and used as the input and output to develop the ANN model. The results show that the performance of the activation function MLP neural network gives a better result. This paper employs three activation functions, hyperbolic tangent sigmoid (tan-sig), logistic sigmoid (log-sig), and linear, to train and test in both two hidden layers and three hidden layers. Log g-sig emerges as the optimal activation function and technique following training and testing in the system with two hidden layers. In comparison, when three hidden layers are used, logistic sigmoid connected with linear is the best calibration because it produces less root means square (RMS) error than the other activation functions.

The graph in Figure 5 illustrates the correlation between the log-sig and linear functions. In the case of two hidden layers using log-sig, the root mean square error (RMSE) is recorded at 0.1248. Conversely, when combining log-sig and linear in the hidden layers, the RMSE is slightly lower at 0.1158. For three hidden layers employing log-sig, the RMSE value increases to 0.2025, while the combination of log-sig, linear, and log-sig in the layers results in an RMSE of 0.051.

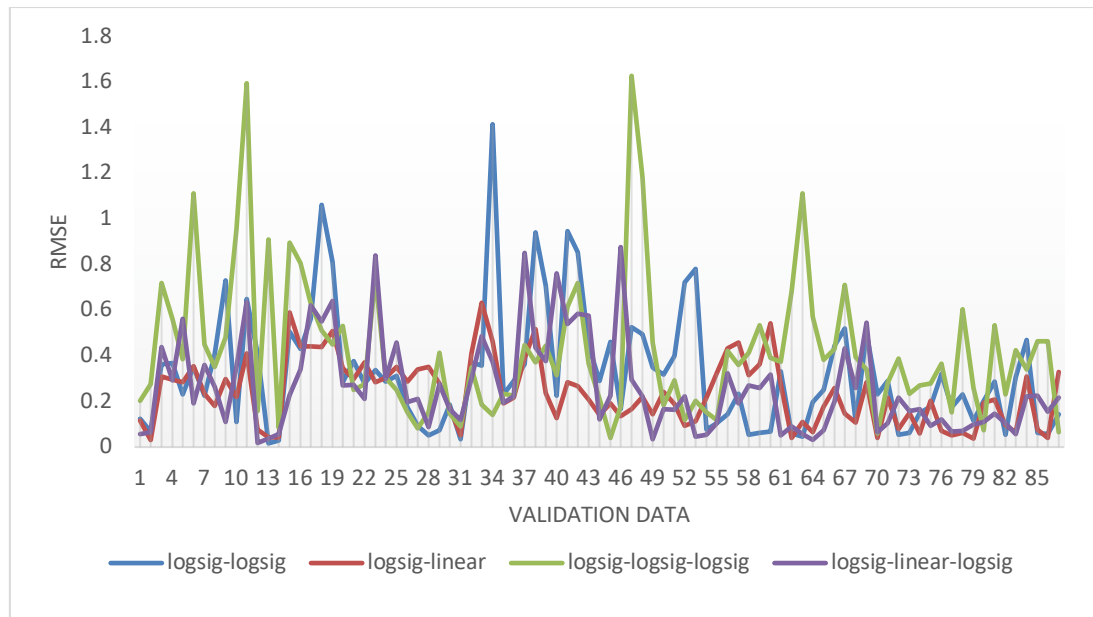


**Fig. 5.** Comparison between different types and numbers of layers with the result of RMS errors in logistic sigmoid (log-sig) and linear

Figure 6 depicts the relationship between the linear and logistic sigmoid functions. In the scenario of two hidden layers utilizing linear functions exclusively, the RMSE is recorded at 0.143. On the other hand, when combining linear and log-sig in the hidden layers, the RMSE value increases to 0.224. Meanwhile, in the case of three hidden layers consisting of linear-log-sig-linear, the RMSE value is measured at 0.146.

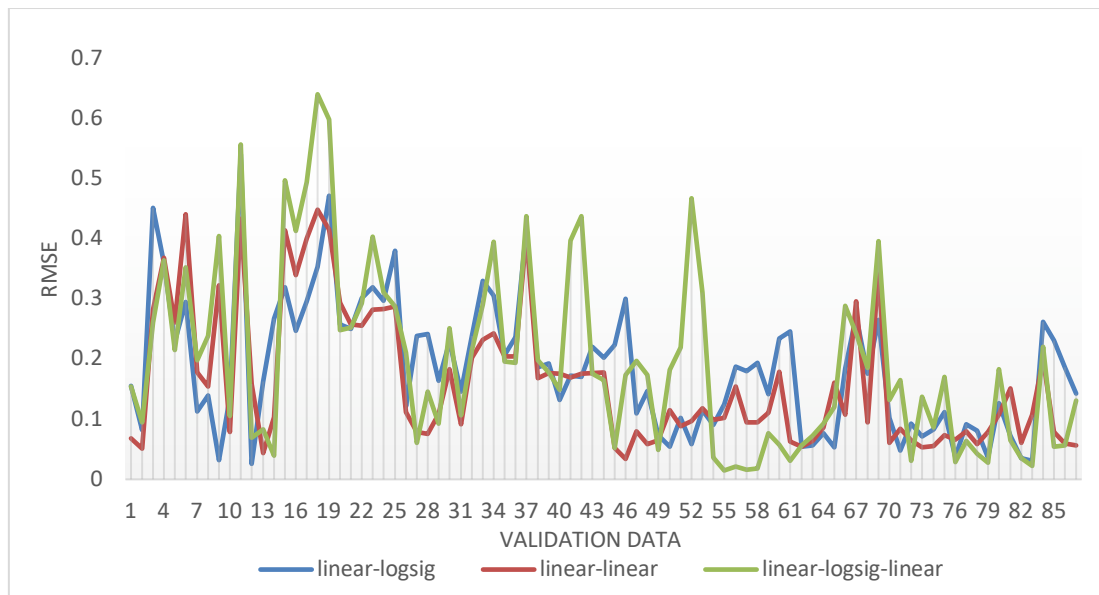


**Fig. 6.** Comparison between different types and numbers of layers with the result of RMS errors in linear and logistic sigmoid (log-sig)

When comparing the root mean square error (RMSE) for hyperbolic tangent sigmoid and linear functions in Figure 7, the configuration with 2 hidden layers using tan-sig-linear exhibits an RMSE of 0.153. In contrast, the tan-sig configuration yields a slightly higher RMSE value of 0.228. Moving to 3 hidden layers with the sequence tan-sig-linear-tan-sig, the RMSE is further elevated to 0.239. Upon

evaluating all the graphs and RMSE values for each group of transfer functions in both 2 and 3 hidden layers, it becomes evident that the transfer function combination yielding the best performance is log-sig-linear-log-sig, achieving a minimal error of 0.051.

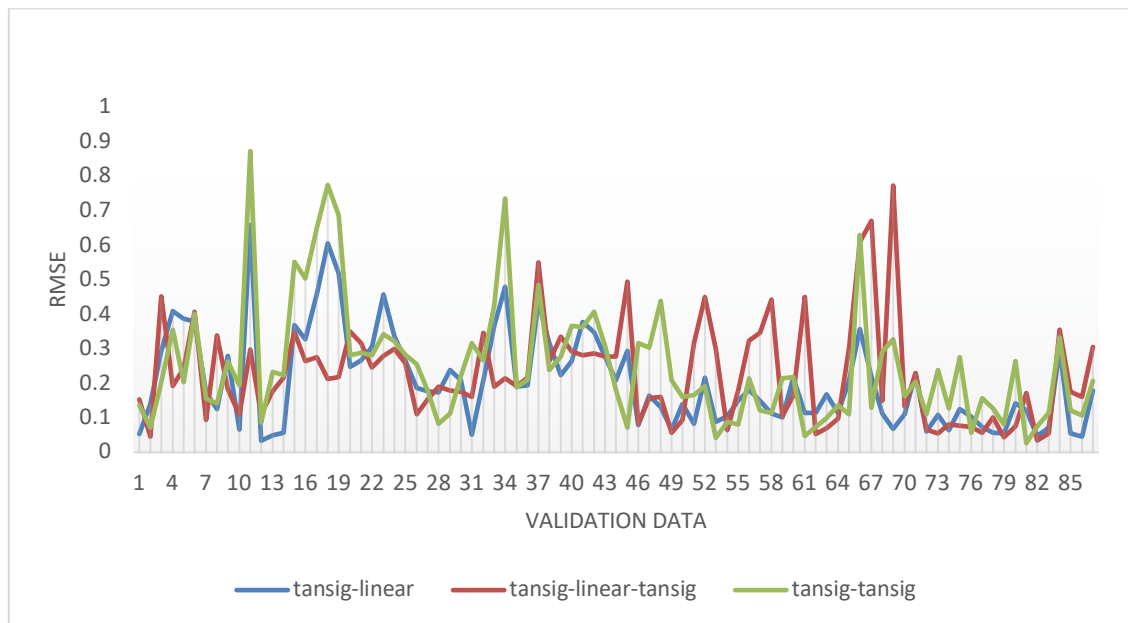


**Fig. 7.** Comparison between different types and numbers of layers with the result of RMS errors in hyperbolic tangent sigmoid (tan-sig) and linear

**Table 5**  
Performance of neural network in the testing stage.

No	Type Of Transfer Function	RMSE
1	Log-sig – Log-sig	0.1248
2	Log-sig – Log-sig – Log-sig	0.2025
3	Log-sig – Linear	0.1158
4	<b>Log-sig – Linear – Log-sig</b>	<b>0.0510</b>
5	Linear– Log-sig	0.2240
6	Linear – Log-sig – Linear	0.1460
7	Linear – Linear	0.1430
8	Tan-sig – Linear	0.1530
9	Tan-sig – Linear – Tan-sig	0.2390
10	Tan-sig – Tan-sig	0.2280

Table 5 summarizes the network error with bold figures representing the best testing RMSE values for each type of transfer function. The transfer function combination of Log-sig – Linear – Log-sig has the lowest testing RMSE value of 0.0510, making it the most accurate configuration among the tested options. The Log-sig – Linear and Linear – Linear configurations also show relatively low RMSE values at 0.1158 and 0.1430, respectively. The Tan-sig – Linear – Tan-sig combination has the highest testing RMSE value of 0.2390, indicating less accuracy than other configurations. In conclusion, the Log-sig – Linear – Log-sig transfer function configuration is recommended for optimal accuracy in predicting the neural network's performance during the testing stage.

#### 4. Conclusion

The ANN method has been implemented to model and predict the output of the PV module. The primary objective is to determine the optimal combination of neuron layers and the most accurate transfer function using MATLAB software. Input and output data sets are recorded in MATLAB to generate a neural network model, which aims to capture the characteristics of PV power systems.

In the hidden layer, various activation functions are considered for the ANN system, including Hyperbolic Tangent Sigmoid, Logistic Sigmoid, and Linear functions. The results obtained from the neural network are analyzed to identify the best function that yields minimal errors. In addition, using 18 neurons in a layer is the most effective configuration for training, testing, and validation, resulting in minimal RMSE.

Furthermore, the study finds that employing a combination of log-sig, linear, and log-sig functions in three hidden layers of MLP provides the best-fitting results with minimal errors. As a recommendation for future improvements, an optimization process could be explored to enhance the accuracy of the prediction model. Additionally, integrating different types of input and output variables and comparing their impact could contribute valuable insights to the study.

#### Acknowledgment

This research was supported by the Ministry of Higher Education (MOHE) through the Fundamental Research Grant Scheme FRGS/1/2022/TK08/UTHM/03/16.

#### References

- [1] Awasthi, Anshul, Akash Kumar Shukla, Murali Manohar S. R., Chandrakant Dondariya, K. N. Shukla, Deepak Porwal, and Geetam Richhariya. "Review on Sun Tracking Technology in Solar PV System." *Energy Reports* 6 (2020): 392–405. <https://doi.org/10.1016/j.egy.2020.02.004>.
- [2] International Energy Agency (IEA). Accessed November 2023. <https://www.iea.org/>.
- [3] Energy Commission. *Malaysia Energy Statistics Handbook 2020*. ISSN 2289-6953. ST(P)03/03/2021.
- [4] Jaber, M., A. S. Abd Hamid, K. Sopian, A. Fazlisan, and A. Ibrahim. "Prediction Model for the Performance of Different PV Modules Using Artificial Neural Networks." *Applied Sciences* 12 (2022): 3349. <https://doi.org/10.3390/app12073349>.
- [5] Bugaje, Aminu, Akhilesh Yadav, Kedar Mehta, Felicia Ojinji, Mathias Ehrenwirth, Christoph Trinkl, and Wilfried Zörner. "Influence of Input Parameters on Artificial Neural Networks for Off-Grid Solar Photovoltaic Power Forecasting." In *NEIS Conference 2021*, Hamburg, September 13–14, 2021. ISBN 978-3-8007-5651-3.
- [6] Kim, EunGyeong, M. Shaheer Akhtar, and O-Bong Yang. "Designing Solar Power Generation Output Forecasting Methods Using Time Series Algorithms." *Electric Power Systems Research* 216 (2023): 109073. <https://doi.org/10.1016/j.epsr.2022.109073>.
- [7] Hou, Xinxing, Chao Ju, and Bo Wang. "Prediction of Solar Irradiance Using Convolutional Neural Network and Attention Mechanism-Based Long Short-Term Memory Network Based on Similar Day Analysis and an Attention Mechanism." *Heliyon* 9 (2023): e21484. <https://doi.org/10.1016/j.heliyon.2023.e21484>.
- [8] Nejati, M., and N. Amjady. "A New Solar Power Prediction Method Based on Feature Clustering and Hybrid-Classification Regression Forecasting." *IEEE Transactions on Sustainable Energy* 13 (2022): 1188–1198. <https://doi.org/10.1109/tste.2021.3138592>.
- [9] Sun, M., C. Feng, and J. Zhang. "Probabilistic Solar Power Forecasting Based on Weather Scenario Generation." *Applied Energy* 266 (2020): 114823. <https://doi.org/10.1016/j.apenergy.2020.114823>.
- [10] Lara-Benítez, P., M. Carranza-García, J. M. Luna-Romera, et al. "Short-Term Solar Irradiance Forecasting in Streaming with Deep Learning." *Neurocomputing* 546 (2023): 126312. <https://doi.org/10.1016/j.neucom.2023.126312>.
- [11] Banik, Rita, and Ankur Biswas. "Improving Solar PV Prediction Performance with RF-CatBoost Ensemble: A Robust and Complementary Approach." *Renewable Energy Focus* 46 (2023): 207–221. <https://doi.org/10.1016/j.ref.2023.06.009>.
- [12] Wen, H., Y. Du, X. Chen, et al. "A Regional Solar Forecasting Approach Using Generative Adversarial Networks with Solar Irradiance Maps." *Renewable Energy* 216 (2023): 119043. <https://doi.org/10.1016/j.renene.2023.119043>.

- [13] Lee, Joonyoung, and Jonghan Jin. "A Novel Method to Design and Evaluate Artificial Neural Network for Thin Film Thickness Measurement Traceable to the Length Standard." *Scientific Reports* 12 (2022): 2212. <https://doi.org/10.1038/s41598-022-06247-y>.
- [14] Ansari, Md Tabish, and M. Ridzuan. "ANN and PSO-Based Approach for Solar Energy Forecasting: A Step Forward Sustainable Energy Generation." In *2021 4th International Conference on Recent Development in Control, Automation & Power Engineering (RDCAPE)*, 2021. <https://doi.org/10.1109/RDCAPE52977.2021.9633719>.
- [15] Olab, A. G., Mohammad Ali Abdelkareem, Concetta Semeraro, Muaz Al Radi, Hegazy Rezk, Omar Muhaisen, Omar Adil Al-Isawi, and Enas Taha Sayed. "Artificial Neural Networks Applications in Partially Shaded PV Systems." *Thermal Science and Engineering Progress* 37 (2023): 101612. <https://doi.org/10.1016/j.tsep.2022.101612>.
- [16] Ilbeigi, Marjan, Mohammad Ghomeishi, and Ali Dehghanbanadaki. "Prediction and Optimization of Energy Consumption in an Office Building Using Artificial Neural Network and a Genetic Algorithm." *Sustainable Cities and Society* 61 (2020): 102325. <https://doi.org/10.1016/j.scs.2020.102325>.
- [17] AlShafeey, Mutaz, and Csaba Csáki. "Evaluating Neural Network and Linear Regression Photovoltaic Power Forecasting Models Based on Different Input Methods." *Energy Reports* 7 (2021): 7601–7614. <https://doi.org/10.1016/j.egy.2021.10.125>.
- [18] Khan, Muhammad Adnan, Ahmed Mohammed Saleh, Muhammad Waseem, and Intisar Ali Sajjad. "Artificial Intelligence Enabled Demand Response: Prospects and Challenges in Smart Grid Environment." *IEEE Access* 11 (2023). <https://doi.org/10.1109/ACCESS.2022.3231444>.
- [19] Mahdi, Berivan H., Kamil M. Yousif, and Luqman M. S. Dosky. "Using Artificial Neural Networks to Predict Solar Radiation for Duhok City, Iraq." In *2020 International Conference on Computer Science and Software Engineering (CSASE)*, Duhok, Iraq. <https://doi.org/10.1109/CSASE48920.2020.9142119>.
- [20] Musa, Aminu, and Farouq Aliyu. "Performance Evaluation of Multi-Layer Perceptron (MLP) and Radial Basis Function (RBF)." In *2019 2nd International Conference of the IEEE Nigeria Computer Chapter (NigeriaComputConf)*. <https://doi.org/10.1109/NigeriaComputConf45974.2019.8949669>.
- [21] Huang, Hailong, Shahab S. Band, Hojat Karami, Mohammad Ehteram, Kwok-Wing Chau, and Qian Zhang. "Solar Radiation Prediction Using Improved Soft Computing Models for Semi-Arid, Slightly-Arid and Humid Climates." *Alexandria Engineering Journal* 61 (2022): 10631–10657. <https://doi.org/10.1016/j.aej.2022.03.078>.
- [22] Kılıç, Fatih, Ibrahim Halil Yılmaz, and Ozge Kaya. "Adaptive Co-Optimization of Artificial Neural Networks Using an Evolutionary Algorithm for Global Radiation Forecasting." *Renewable Energy* 171 (2021): 176–190. <https://doi.org/10.1016/j.renene.2021.02.074>.
- [23] Zaaoumi, Anass, Zahra Bouramdane, Abdellah Bah, Mohammed Alaoui, and Abdellah Mechaqrane. "Energy Production Estimation of a Parabolic Trough Solar Power Plant Using Artificial Neural Network." In *4th International Conference on Electrical and Information Technologies (ICEIT 2020)*. <https://doi.org/10.1109/ICEIT48248.2020.9113176>.
- [24] Tavares, Ines, Ricardo Manfredini, Jose Almeida, Joao Soares, Sergio Ramos, Zahra Forooshandeh, and Zita Vale. "Comparison of PV Generation Forecasting in a Residential Building Using ANN and DNN." *IFAC PapersOnLine* 55, no. 9 (2022): 291–296. <https://doi.org/10.1016/j.ifacol.2022.07.051>.
- [25] AbdulBaqi, Faten Khalid, and Khudhur R. Abdulrahman. "The Effect of Humidity, Temperature, and Total Solar Radiation on the Efficiency of Polycrystalline Solar Panel." *Diyala Journal for Pure Science* (July 2021). <https://www.researchgate.net/publication/354100395>.